Technique with lock-in amplifier for real-time measurement of tricuspid valve annulus area

KOUICHI TAMIYA, MASAFUMI HIGASHIDATE, AND SHO KIKKAWA
Departments of Surgical Science and Pediatric Cardiovascular Surgery, The Heart Institute of Japan, Tokyo Women's Medical College, Tokyo 162, Japan

TAMIYA, KOUICHI, MASAFUMI HIGASHIDATE, AND SHO KIKKAWA. *Technique with lock-in amplifier for real-time measurement of tricuspid valve annulus area.* Am. J. Physiol. 251 (Heart Circ. Physiol. 20): H236–H241, 1986.—A new measuring system that permits real-time registration of the tricuspid valve annular area (TV*A*) using lock-in amplifier is devised and applied in open-chest anesthetized dogs. The tricuspid valve annulus was stitched with a fine, pliable, metal thread made of 10 30-μm urethane resin-coated copper wires during inflow occlusion. Both ends of the thread were guided out from the right atrium through a single pinhole in the right atrial wall. The signal intensity induced in the sense loop is linearly related to the area encircled by the thread, i.e., the area of the tricuspid annulus. During control state, TV*A* varied by an average of 24.5% (3.8–46.5%) of its maximum. Presystolic peak and valley of TV*A* due to atrial contraction and a decrease in TV*A* during ventricular ejection were generally observed. An increase in TV*A* during the initial portion of isovolumic contraction phase was prominent in dogs with filariasis, whereas in the other dogs it was not.

tricuspid regurgitation; pulmonary hypertension; atrial contribution to ventricular filling

THE ATRIOVENTRICULAR VALVE ANNULUS demonstrates a changing size during the cardiac cycle on fluoroscopic video images (2, 8, 9). This change is considered to be an important factor influencing appropriate valve closure and effective ventricular filling. There has been no direct technique available for real-time measurement of the area of the atrioventricular valve annulus with sufficient reliability. Recently, a noninvasive technique was introduced which permits the determination of the atrioventricular valve annular area in human beings by use of two-dimensional echocardiography (5, 7). This method requires reconstruction of the contour of the valve annulus from multiple planes taken at various phases and with interval changes in transducer rotation. In addition, inherent inaccuracy related to the ambiguity of the sound reflecting loci of moving objects prevents wide application of this technique to the registration of the phasic variations in the size of the atrioventricular valve annulus.

The present report describes a new method utilizing lock-in amplification to pick up the small signal with an one-turn loop stitched along the tricuspid valve annulus in open-chest anesthetized dogs. This method yields quantitative information of atrioventricular valve annular area with superb signal-to-noise ratio and reasonable frequency response.

MATERIALS AND METHODS

Measuring system. The equipment we have devised for monitoring the tricuspid valve annular area (TV*A*) is based on electromagnetic induction (3). Three alternating electromagnetic fields of different frequency are provided in the region of the tricuspid valve annulus that is encircled with fine pliable metal thread (diameter 0.2–0.3 mm) made of 10 30-μm urethane resin-coated copper wires. The magnitude of the alternating electric potential (about 5–10 μV) containing three signals induced in a sense loop is proportional to the area enclosed under conditions of constant electromagnetic field; this area is predominantly that of the tricuspid annulus.

The block diagram of the electronic circuitry designed for the present study is shown in Fig. 1. Three quadrature oscillators generate 96-, 100-, and 104-kHz sine wave signals, which are utilized as carrier signals. These signals are supplied for three power amplifiers. Each power amplifier provides a 30-W sine wave for each drive coil made of 0.5-mm enamel wire. Three drive coils, the axes of which intersect with each other at vertically opposite angles of 20°, were assembled on a plywood platform (Fig. 1). The one-turn sense loop, which works as a receiving antenna for the three carrier signals, is connected to a preamplifier made of a high-frequency operational amplifier (Signetics NE592) with a short segment of fine shielded wire. The amplified signal is put into three phase-sensitive detectors, which are directly supplied with three individual carrier signals from the three carrier oscillators. The combination of a phase-sensitive detector (Analog Devices AD630JN) and a low-pass filter (Burr-Brown UAF41) acts as a lock-in amplifier that functions as a very stable and narrow band-pass filter and a precise detector combined. The system described here has an excellent signal-to-noise ratio in the presence of large amounts of uncorrelated noise. Three low-pass filters have specifications of Butterworth response, 50-Hz cutoff frequency, and −18 dB/oct gain slope. The area signal is not considered to have a frequency component above 30 Hz. The calculation of project area of the sense loop to the drive coil base from three signals showed that the errors due to axis deviation during

0363-6135/86 $1.50 Copyright © 1986 the American Physiological Society

contraction were insignificant (see APPENDIX). The final stage of the measuring system consists of an operational amplifier (National Semiconductors LF356), which acts as a summing invertor and an offset adjuster combined.

Calibration procedure. The linearity test of the system was performed outside of the animal by use of a short-circuit (for 0) and four glass cylinders of known diameter mounted on a pan head. The relation between the areas formed by wrapping a metal thread around the cylinders and the magnitude of output voltage measured with a 4.5-digit digital voltmeter (VOAC-747 Iwatsu) is shown in Fig. 2. The linearity of the measuring system is found to be very high, and the offset voltage was compensated with the offset adjuster. Changes in output voltage during sense loop immersion in isotonic saline was so small (+2.0 to approx. −1.7% at most) that correction for a calibration factor, due to changes in conductivity of the medium around the sense loop, was unnecessary. The relation between the angle of the sense loop to the platform of the drive coil assembly and the amplitude of the output signal is also shown in Fig. 2. These data

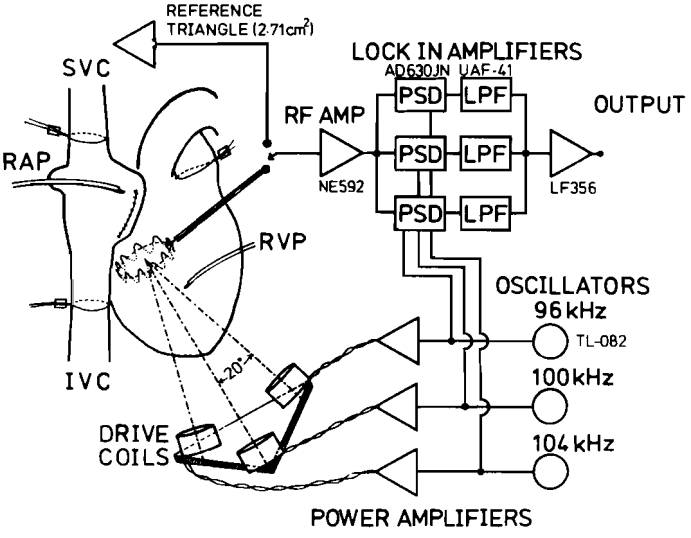

FIG. 1. Experimental setup and block diagram of electronic circuitry designed for the present study. PSD, phase-sensitive detector; LPF, low-pass filter; RAP, right atrial pressure; RVP, right ventricular pressure; RF AMP, radio-frequency amplifier.

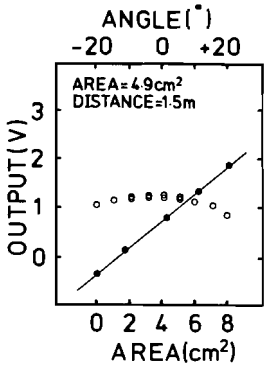

FIG. 2. Relation between area encircled with sense loop and output voltage (*closed circles*, $Y = 0.25X - 0.24$, $R = 0.999$) and relation between the angle of sense loop to the base of drive coil (*open circles*) measured with a voltmeter. Distance between drive coil assembly and sense loop was held at 1.5 m.

indicate that the errors caused by the deviation of the sense loop axis from the perpendicular extension of the drive coil platform within ±10° can be ignored. According to the computation of the angle of the tricuspid valve plane to the drive coil platform (see APPENDIX), axis deviation throughout systole and diastole was estimated at 6.1° at most. A metal triangle, which was constructed with three rigid brass rods (1 mm diameter, 2.5 cm length), provided a standard area signal (2.71 cm^2) for the measuring system whenever the reference signal was required during the animal experiment. This triangle for calibration was connected to the preamplifier in place of the fine metal thread loop that was stitched along the tricuspid annulus. It was placed at the tricuspid valve region adjacent to the heart and at a distance of 0.8 to approximately 1.0 m from the drive coil assembly. Zero level was adjusted by connecting a short circuit in place of the sense loop. During calibration procedure, the plane of the triangle was adjusted to be parallel with the platform of the drive coil assembly by rotating the triangle manually so that the three frequency signals showed equal intensity.

Sense loop installation. The dogs were anesthetized with intravenous pentobarbital sodium (30 mg/kg). After artificial ventilation was established, a right thoracotomy at the fourth intercostal space or a median sternotomy was carried out. The azygous vein was ligated, then the superior and inferior venae cavae were occluded with two snares. After the right atrial incision was made, a metal thread consisting of 10 urethane resin-coated copper wires (Sumitomo Denko, 30-μm Uremett wire), which functions as a sense loop of the electromagnetic fields, was stitched along the tricuspid annulus (visible juncture of the valve leaflets and the cardiac wall). To accommodate changes in circumferential length of the valve ring, the metal string was introduced into the myocardium along the valve ring with gathered stitches (Fig. 1). Every 90 s of inflow occlusion, the right atrium was temporarily closed and venous inflow occlusion was released. Thus the sense loop installation procedure was divided into three or four segments. Both ends of the string were guided out from the right atrium through a single pinhole in the right atrial wall and were tightly twisted. To eliminate extra loop formation of the string in the right atrium, both ends of the metal thread were pulled gently by hand, then connected to the high-frequency preamplifier with a piece of shielded wire by soldering. After a visual confirmation of appropriate arrangement of the sense loop along the valve annulus in the atrium, the incision in the right atrium was sutured, then the blood circulation was reestablished. The twisted lead wires were fixed with cyanoacrylate glue to avoid extra loop area formation. The drive coil assembly was placed perpendicular to the extension of the long axis of the heart and was directed toward the tricuspid valve region.

Experimental protocol. Right ventricular pressure (RVP), right atrial pressure (RAP), and TV*A* were monitored simultaneously by use of two catheter-tipped manometers (Millar PC-370). Aortic pressure and standard lead II electrocardiogram (ECG II) were recorded conventionally throughout the experiment. Measurements

TABLE 1. *Area of tricuspid annulus and hemodynamic parameters in nine dogs*

Dog	Body Wt, kg	Heart Rate, beats/min	RVP, mmHg	Values of Area of Tricuspid Valve Annulus, cm^2				Pulmonary stenosis
				Control	Inflow occlusion	Isoproterenol, 1 μg	Saline, 200-ml infusion	
							Before → After	
1	17	128	24	3.18/2.46	2.37/2.03	3.38/2.23 (166)		
*2**	15	100	20	1.98/1.22	0.86/0.65	1.91/1.12 (132)	2.30/1.62 → 2.43/2.36	
3	22	95	25	4.32/2.30	3.04/0.67	4.20/2.30 (144)	4.50/3.11 → 4.33/3.79	
*4**	16	103	17	2.57/2.30		2.70/2.10 (125)		3.38/2.92
5	14	129	25	3.14/2.16		2.98/1.89 (130)	3.07/1.96 → 3.52/2.57	5.82/3.99
6	19	140	38	3.32/1.96	2.16/1.22	2.84/1.69 (162)	3.25/2.03 → 3.52/2.84	4.06/2.37
7	20	113	20	3.38/3.25	2.71/2.30	3.79/3.11 (162)	3.92/3.38 → 4.19/3.79	4.60/3.79
8	21	136	19	2.64/2.44	1.89/1.49	2.84/2.16 (150)	3.25/2.84 → 3.65/3.24	3.92/2.84
9	15	88	32	4.80/4.06	2.10/1.35	4.19/3.38 (96)	5.00/4.19 → 5.27/4.39	5.41/4.74
Mean	17.7	114.7	24.44	3.26/2.46	2.16/1.39	3.20/2.22 140.11	3.61/2.73	3.84/3.28	4.53/3.44
±SD	2.9	19.1	6.77	0.87 0.08	0.69 0.63	0.76 0.69 24.11	0.92 0.92	0.88 0.74	0.93 0.88

Values of area of tricuspid valve annulus are denoted as maximum/minimum values, respectively. Values in parentheses denote heart rates after isoproterenol administration. RVP, right ventricular pressure. * Dogs without filariasis.

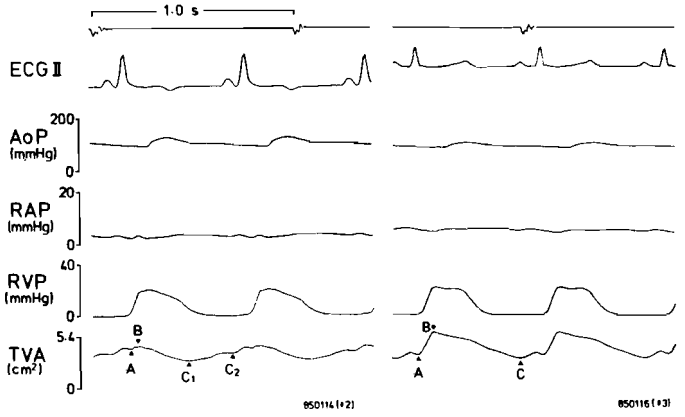

FIG. 3. Two representative recordings of lead II electrocardiogram (ECG II), aortic pressure (AoP), right atrial pressure (RAP), right ventricular pressure (RVP), and tricuspid valve annular area (TV*A*). *Left*, recorded from a dog that did not have filariasis. *Right*, recorded from a dog with filariasis. *A–C*, see text.

were taken at end-expiratory points. Polarity was adjusted such that a downward deflection indicated reduction in TV*A*. To test the effects of enhanced myocardial contractility on TV*A*, isoproterenol (1 μg) was administered intravenously. To evaluate the effects of increased right ventricular preload and total load on TV*A*, a rapid saline infusion (200 or 300 ml within 5 min) and partial constriction of the main pulmonary artery were performed at the end of each experiment. The parameters relevant to changes in TV*A* are summarized in Table 1. In several experiments, administration of acetylcholine chloride (50 mg) or electrical stimulation of the right cervical vagus nerve were carried out to evaluate the effects of arrhythmia, isolated ventricular contraction, and isolated atrial contraction.

RESULTS

A presystolic peak of TV*A* was observed in ventricular systoles with preceding atrial systole ~75 ms after the onset of the P wave. On the other hand, the isolated atrial contraction during ventricular asystole produced a downward deflection of TV*A* ~160 ms after the onset of the P wave. The valley of the TV*A* (in Fig. 3*A* and Fig. 5) also appeared ~160 ms after the onset of the P wave.

In two dogs (*nos. 2* and *4*) without filariasis, who had small TV*A* values with respect to their body weights, a slight increase in TV*A* during the isovolumic contraction phase was observed (Fig. 3, *A* and *B*, left). In seven dogs that had filariasis, the enlargement of TV*A* during the isovolumic contraction phase was more prominent (Fig. 3, *A* and *B*, right). In both cases, TV*A* progressively decreased during the right ventricular ejection phase. The valley of TV*A* during ventricular relaxation was tentatively labeled *point C*, in Fig. 3. If two valleys appeared during the relaxation phase, these valleys were labeled C_1 and C_2, respectively (Fig. 3, left, and Fig. 5). The slow recordings of TV*A* and other relevant hemodynamic parameters are demonstrated in Fig. 4.

Effects of inflow occlusion. During a brief inflow occlusion, TV*A* decreased significantly, but was still fluctuating around one-half of its control value.

Effects of isoproterenol administration. The bolus administration of isoproterenol (1 μg) produced an increase in heart rate and RVP, a slight decrease in aortic pressure, and little change in mean TV*A*, as shown in Fig. 4.

Combined effects of volume loading and arrhythmia induced by acetylcholine. To observe the effect of an isolated ventricular systole on TV*A*, ventricular extrasystoles were produced by the administration of acetylcholine chloride (50 mg), which is said to cause a pulmonary vasodilation, after a rapid infusion of 300 ml of isotonic saline. The combination of increased preload and arrhythmia without preceding atrial systole produced distinct RAP elevation during ventricular systole, which suggested tricuspid regurgitation. An appropriate atrial contraction not only prevented the regurgitation in the third and fourth cardiac cycles in Fig. 5, in which abnormal RAP elevation presumably due to regurgitation was absent, but also brought about an ~5% reduction in TV*A* at *point A* in Fig. 5. In the present experiment, tricuspid regurgitation was not confirmed; however, it is likely that an appropriate atrial contraction would reduce the possibility of the tricuspid regurgitation.

DISCUSSION

The electromagnetic induction method utilizing lock-in amplification described here makes it possible to re-

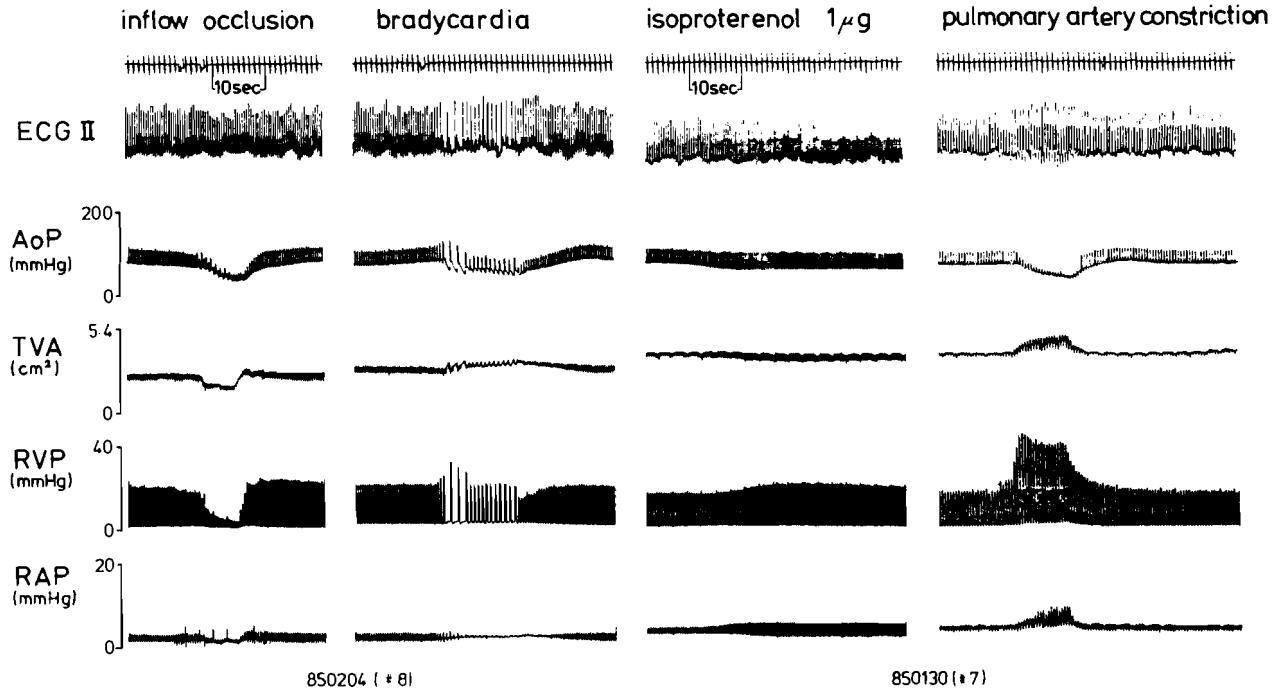

FIG. 4. Slow recordings of TV*A* and relevant hemodynamic parameters during (from the left most column) inflow occlusion, bradycardia induced by vagus nerve stimulation, isoproterenol infusion, and mechanical pulmonary artery constriction. See Fig. 3 for abbreviations.

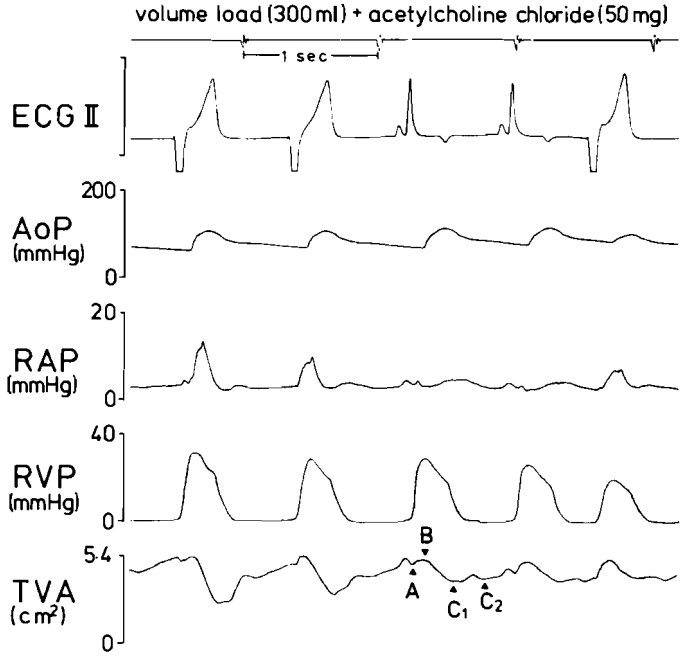

FIG. 5. Recordings of TV*A* and other hemodynamic parameters during acetylcholine chloride administration after volume loading. Note distinct RAP elevation in the 1st, 2nd, and 5th contractions that suggests tricuspid regurgitation during extra ventricular systoles. See Fig. 3 for abbreviations.

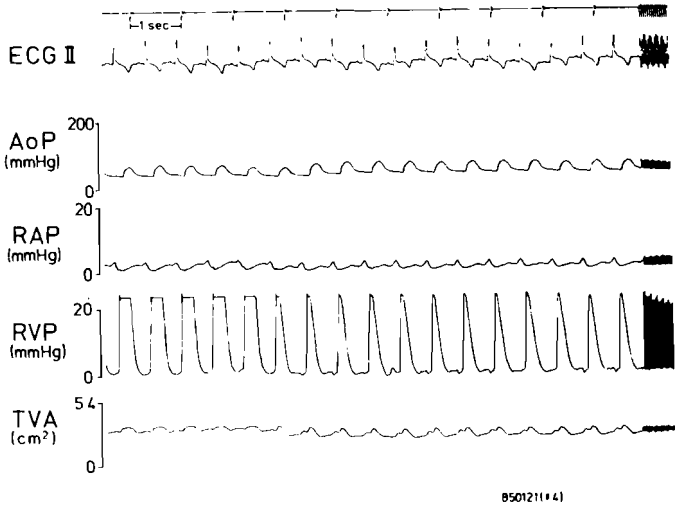

FIG. 6. Representative trace of TV*A* and other hemodynamic parameters during gradual release of pulmonary artery constriction. Note changes in TV*A* pattern during gradual release of outflow constriction. See Fig. 3 for abbreviations.

cord phasic variations of the tricuspid valve annulus under conditions of physiological RAP, RVP, and blood flow. The sense loop stitched along the valve annulus is not only so light but also so pliant that it will cause minimal disturbance to the free movement of the tricuspid annulus. Since autopsy showed that the metal thread was appropriately stitched along the tricuspid valve ring with 15–18 points, movement of the annulus was considered to be free from restraint, and the area enclosed by the metal thread must represent that of the tricuspid valve annulus. In addition to the merits such as high accuracy, high signal-to-noise ratio, direct calibration, and minimal disturbance to the valve movement, the electrical source impedance of the signal is so low that the output signal of TV*A* was insensitive to insulation breakage or changes in conductivity of the surrounding medium of the sense loop. Actually, only direct metal

contact between lead wires altered the magnitude of the area signal. In addition to the excellent sensitivity and accuracy of the present method, the equipment necessary for the present method can easily be handmade in a laboratory from inexpensive electrical parts that are commonly available.

Tsakiris et al. (9) referred to a brief increase in the tricuspid valve area that appeared between the ECG P and Q waves at slower heart rates. The presystolic peak observed in the present study may correspond to it. This presystolic peak and valley seemed to be a characteristic feature of the phasic variations in the atrioventricular valve ring during normal sinus rhythm. The squeezing action of atrial systole or so-called 'atrial kick' must enlarge the TV*A* first, then the propagation of atrial systole to the base of the atrium must reduce it, since it did not appear in cardiac cycles without preceding atrial systole (the first and second cardiac cycles in Fig. 5). Tsakiris et al. (8, 9) emphasized that a large portion (approximately two-thirds) of the total decrease in size of the annulus occurred prior to the onset of ventricular contraction in anesthetized closed-chest dogs. In our experiments, atrial contraction produced a distinct downward notch on TV*A* trace (*point A*), but the reduction in TV*A* in this phase was not so predominant.

Concerning the increase in TV*A* coinciding with right ventricular pressure rise that Tsakiris et al. (8, 9) suggested to exist in both mitral and tricuspid valves, a small but distinct peak of TV*A* at the onset of ventricular pressure rise (ventricular component) was observed in dogs without filariasis in the present study. Instead of the remarkable decrease in TV*A* in the early isovolumic contraction phase due to atrial systole reported by Tsakiris et al. (8, 9), a distinct increase in TV*A* at early systole was observed (Fig. 3, *A* and *B*, right) in dogs whose hemodynamic data suggested pulmonary hypertension due to filariasis. The difference between these two studies may be related to the following different physiological conditions: *1*) our anesthetized open-chest dogs were artificially ventilated with positive pressure; and *2*) a major portion of our experimental animal population had filariasis. The upward ventricular component during the early isovolumic contraction phase in the dogs supposed to have pulmonary hypertension is interesting in conjunction with the effect of pulmonary constriction on TV*A* (Fig. 6). The response to increased outflow resistance is consistent with the finding of Tsakiris et al. (8) in the mitral valve, which is demonstrated in Fig. 10 of their article in which they ascribed the enlargement of annular size to increased atrial size. In Fig. 3, the TV*A* pattern is different under conditions of identical RVP peaks but differing RVP shapes. Although we have no information on the atrial size, the idea that increased outflow resistance or increased ventricular pressure may cause a systolic enlargement of TV*A* seems to be reasonable. In our experiment, a biphasic increase in TV*A* during diastole, which was demonstrated for the tricuspid valve by Tei et al. (7), was frequently observed. The relaxation of the ventricle (reduction in wall stress itself) may be responsible for C_1, since it always appears during the isovolumic relaxation phase, and atrial volume change due to transtricuspid blood flow may produce C_2 during the ventricular filling phase. However, the causes of two downward deflections of TV*A* during the relaxation phase is still unknown. In Fig. 5, atrial systole seemed to effectively prevent the tricuspid regurgitation, but it is still unclear whether this is accomplished through its hemodynamic effect, such as atrial pressure fall due to atrial relaxation, or through its reducing effect of TV*A* (1).

One of the disadvantages of the present method, common to the devices utilizing electromagnetic induction, is interference with the square-wave electromagnetic flowmeter. The insertion of three narrow band-pass filters, which pass only the carrier signals, between the preamplifier and the phase-sensitive detector will effectively minimize the interference. In the present measuring system, we utilized three frequency signals around 100 kHz, of which attenuation in biological tissue or blood is negligible. The adoption of a triangulation procedure not only ensures the appropriate arrangement of the drive coil assembly by monitoring the balance among three signals, but also provides the angle of the sense loop plane to the base of the drive coil assembly through simple calculation from the three signal intensities (see APPENDIX). Conventionally, the measurement of the intracardiac valve annular area has been carried out on fluoroscopic images (2, 8, 9). To obtain a clear configuration of the valve ring, it is necessary to use a large number of radiopaque markers, which because of their weight probably prevents free movement of the valve annulus. Furthermore, improvement of the frequency response of the area signal by use of that technique requires an expensive high-speed cinefluoroscopic system. On the other hand, the determination of the valve annulus by use of two-dimensional echocardiography has the great advantage of noninvasive measurement (4–7); however, the accuracy of the measurement is open to criticism. The present area measuring system, which is applicable to other organs, should provide a significant extension of area monitoring for physiological animal studies at minimum expense.

APPENDIX

When the three drive coils are arranged such that the axes of the coils intersect, ~1 m from the sense loop, at the vertically opposite angle of θ (20° was chosen in our study as a compromise between accuracy and portability), *Eq. 1* provides the project area of the sense loop to the base of the drive coil assembly.

$$s = \sqrt{\frac{(x^2 + y^2 + z^2)\,(1 + \cos\theta) - 2\,(xy + yz + zx)\cdot\cos\theta}{(1 - \cos\theta)\,(1 + 2\cos\theta)}} \qquad (1)$$

where s denotes the project area of the sense loop to the drive coil base, x, y, and z denote the intensities of three carrier signals, θ denotes the vertical angle of the axes of the three drive coils. *Equation 2* gives the tricuspid valve axis angles to the three axes of the drive coils.

$$a = \cos^{-1}\left(\frac{x}{s}\right),\ b = \cos^{-1}\left(\frac{y}{s}\right),\ c = \cos^{-1}\left(\frac{z}{s}\right) \qquad (2)$$

where a, b, and c denote the angles of the valve axis to the three axes of drive coils.

For example, three signal intensities at minimum TV*A* during systole were 2.29, 2.35, and 2.41 cm^2, and those at maximum TV*A* were

2.71, 2.75, and 2.79, respectively. The ratio of minimum/maximum TV*A* values calculated from *Eq. 1* was 0.858 (2.42 cm^2/2.82 cm^2), and that of minimum/maximum TV*A* values calculated as an arithmetic mean of three carrier intensities from simultaneously registered signals was 0.855 (2.35 cm^2/2.75 cm^2). The errors caused by the adoption of arithmetic mean was estimated ~0.3% of the maximum value of TV*A*. On the other hand, the angles of valve plane axis were calculated as follows: $a = 15.8°$, $b = 12.5°$, and $c = 7.9°$ at maximum TV*A*; $a = 19.1°$, $b = 14.1°$, and $c = 6.0°$ at minimum TV*A* during systole. Therefore, maximum axis deviation during the cardiac cycle was 3.3° in this case. The maximum axis deviation observed was 6.1°, at most, throughout the experiment.

The authors are grateful to the members of the animal laboratory of The Heart Institute of Japan for their expert help and hearty encouragement and to Yuko Yoshino for her secretarial assistance. We also acknowledge the contribution of Hideki Sawaguchi of the Waseda University.

Address for reprint requests: K. Tamiya, Dept. of Surgical Science, The Heart Institute of Japan, Tokyo Women's Medical College, 8-1 Kawadacho, Shinjuku Tokyo 162, Japan.

Received 15 April 1985; accepted in final form 5 March 1986.

REFERENCES

1. BRAUNWALD, E., S. D. ROCKOFF, H. N. OLDHAM, JR., AND J. ROSS, JR. Effective closure of the mitral valve without atrial systole. *Circulation* 33: 404–409, 1966.
2. DAVIS, P. K. B., AND J. B. KINMONTH. The movements of the annulus of the mitral valve. *J. Cardiovasc. Surg.* 4: 427–431, 1963.
3. HUNTSMAN, L. L., D. S. JOSEPH, M. Y. OIYE, AND G. L. NICHOLS. Auxotonic contractions in cardiac muscle segments. *Am. J. Physiol.* 237 (*Heart Circ. Physiol.* 6): H131–H138, 1979.
4. MARTIN, R. P., H. RAKOWSKI, J. H. KLEIMAN, W. BEAVER, E. LONDON, AND R. L. POPP. Reliability and reproducibility of two dimensional echocardiographic measurement of the stenotic mitral valve orifice area. *Am. J. Cardiol.* 43: 560–568, 1979.
5. ORMISTON, J. A., P. M. SHAH, C. TEI, AND M. WONG. Size and motion of the mitral valve annulus in man. I. A two-dimensional echocardiographic method and findings in normal subjects. *Circulation* 64: 113–120, 1981.
6. POLLICK, C., M. PITTMAN, K. FILLY, P. J. FITZGERALD, AND R. L. POPP. Mitral and aortic valve orifice area in normal subjects and in patients with congestive cardiomyopathy: determination by two dimensional echocardiography. *Am. J. Cardiol.* 49: 1191–1196, 1982.
7. TEI, C., J. P. PILGRIM, P. M. SHAH, J. A. ORMISTON, AND M. WONG. The tricuspid valve annulus: Study of size and motion in normal subjects and in patients with tricuspid regurgitation. *Circulation* 66: 665–671, 1982.
8. TSAKIRIS, A. G., G. VON BERNUTH, G. C. RASTELLI, M. J. BOURGEOIS, J. L. TITUS, AND E. H. WOOD. Size and motion of the mitral valve annulus in anesthetized intact dogs. *J. Appl. Physiol.* 30: 611–618, 1971.
9. TSAKIRIS, A. G., D. D. MAIR, S. SEKI, J. L. TITUS, AND E. H. WOOD. Motion of the tricuspid valve annulus in anesthetized intact dogs. *Circ. Res.* 36: 43–48, 1975.